General Disclaimer

One or more of the Following Statements may affect this Document

- This document has been reproduced from the best copy furnished by the organizational source. It is being released in the interest of making available as much information as possible.

- This document may contain data, which exceeds the sheet parameters. It was furnished in this condition by the organizational source and is the best copy available.

- This document may contain tone-on-tone or color graphs, charts and/or pictures, which have been reproduced in black and white.

- This document is paginated as submitted by the original source.

- Portions of this document are not fully legible due to the historical nature of some of the material. However, it is the best reproduction available from the original submission.

NASA Technical Memorandum 83431
AIAA-83-1175

Analytical and Experimental Study of Flow Through an Axial Turbine Stage With a Nonuniform Inlet Radial Temperature Profile

John R. Schwab, Roy G. Stabe,
and Warren J. Whitney
Lewis Research Center
Cleveland, Ohio

Prepared for the
Nineteenth Joint Propulsion Conference
cosponsored by the AIAA, SAE, and ASME
Seattle, Washington, June 27-29, 1983

NASA

ANALYTICAL AND EXPERIMENTAL STUDY OF FLOW THROUGH AN AXIAL TURBINE STAGE WITH A NONUNIFORM INLET RADIAL TEMPERATURE PROFILE

John R. Schwab, Roy G. Stabe, and Warren J. Whitney

National Aeronautics and Space Administration
Lewis Research Center
Cleveland, Ohio

SUMMARY

Analytical and experimental results are presented for a typical nonuniform inlet radial temperature profile through an advanced single-stage axial turbine and compared with the results obtained for a uniform profile. Gas temperature rises of 40 K to 95 K are predicted at the hub and tip corners at the trailing edges of the pressure surfaces in both the stator and rotor due to convection of hot fluid from the mean by secondary flow. The inlet temperature profile is shown to be mixed out at the rotor exit survey plane (2.3 axial chords downstream of the rotor trailing edge) in both the analysis and the experiment. The experimental rotor exit angle profile for the nonuniform inlet temperature profile indicates underturning at the tip caused by increased clearance. Severe underturning also occurs at the mean, both with and without the nonuniform inlet temperature profile. The inviscid rotational flow code used in the analysis fails to predict the underturning at the mean, which may be caused by viscous effects.

E-1722

INTRODUCTION

The majority of turbine aerodynamics investigations have utilized uniform inlet radial temperature profiles in order to simplify the analytical and experimental procedures. However, the uniform profile does not represent the actual conditions at the turbine inlet in an engine, where large radial variations in the gas temperature are produced by the combustor. Since a nonuniform profile must contain some regions with temperatures higher and lower than the mean temperature, distortion or rotation of the temperature profile by secondary flow might influence the development of hot spots on the blades and endwalls. These hot spots can dramatically reduce the life of the turbine.

A research program has been started at the NASA Lewis Research Center to investigate the effects of typical nonuniform inlet radial temperature profiles in axial turbines. This paper presents analytical and experimental results for a typical nonuniform profile through an advanced single-stage axial turbine and compares them with the results obtained for a uniform profile. The inlet radial temperature profile in the experiment was produced by the Combustor Exit Radial Temperature Simulator (CERTS) inlet which injected coolant air through circumferential slots in the hub and tip endwalls upstream of the stator. The coolant flow rates were adjusted such that the measured inlet temperature profile approximated the design profile for the Lewis Research Center High Pressure Facility (HPF) (ref. 1) in terms of local to mean temperature ratio. Radial surveys of total temperature and total pres-

sure were conducted at the stator inlet and rotor exit both with and without CERTS coolant air injection; the rotor exit flow angle was also measured. The analytical results were obtained from a three-dimensional time-marching inviscid rotational flow code (ref. 2) with inlet conditions taken from the experiment. Rotor exit temperature and flow angle profiles were computed for comparison with the experimental results. In addition, contour plots of computed total temperature in the stator and rotor blade passages are presented, along with computed secondary flow vector plots.

SYMBOLS

b	blade height, cm
c_x	blade axial chord, cm
d	diameter, cm
N	rotative speed, rpm
p	pressure, N/m^2
T	temperature, K
s	blade pitch, cm
U	wheel speed, m/sec
V	absolute velocity, m/sec
w	mass flow, kg/sec
W	relative velocity, m/sec
α	absolute swirl angle, deg
β	relative swirl angle, deg
Δh	specific work output, J/kg

Subscripts:

b	blade
cr	critical condition
m	mean
v	vane
0	stator inlet
1	stator exit or rotor inlet
2	rotor exit

Superscripts:

'	absolute total state
"	relative total state

APPARATUS AND PROCEDURE

Turbine Design

The test turbine is a 0.767 scale model of the first stage of a two-stage core turbine designed for a modern high bypass ratio engine. The design criteria were to accommodate the high work, low flow characteristics of this type of turbine and achieve a subsonic design with reasonable blade height. This was accomplished primarily through the use of a flat stator exit flow angle, 75° from axial.

The design velocity diagrams are shown in figure 1. The stator profile and the rotor profiles at the hub, mean, and tip sections are shown in figures 2 and 3, respectively.

The stator is a constant section (untwisted) constant exit angle design. The rotor leading edge was designed to accept the stator exit flow with either zero or a small negative incidence. The rotor exit was designed for free vortex flow. Both rotor and stator leading and trailing edges are large to accept cooling. The test turbine, however, was uncooled.

The turbine test and standard air equivalent conditions are listed in table I.

Test Facility

A photograph of the turbine test facility, which has been described in some detail in reference 3, is shown in figure 4. The turbine inlet air was supplied from the laboratory 40 psig combustion air system. The pressure was controlled with a 10 inch manually operated main valve and a 6 inch automatically controlled bypass valve. The air was heated with 3 can-type combustors using natural gas as fuel. The air flow was measured with a calibrated commercially available venturi meter. The fuel rate was measured with a flow nozzle. After passing through the turbine the air was throttled to the laboratory altitude exhaust system through a 24 inch butterfly valve.

The turbine power was absorbed with an eddy current dynamometer and dissipated, as heat to the cooling water, in the dynamometer stator. The turbine output torque was measured with a brushless rotating torque meter which was installed on the shaft between the turbine and dynamometer. A backup torque measurement was also made on the dynamometer stator. The turbine rotative speed was measured with an electronic counter and a 60-tooth gear which was mounted on the turbine shaft.

CERTS Inlet

The original turbine inlet section shown in figure 5(a) utilized an existing inlet frame (ref. 4). A new inlet frame was designed for the CERTS study which could accommodate the coolant infusion coupling as shown in figure 5(b). This coupling contains the 4 coolant plenums (2 at the hub and 2 at the tip) and the coolant supply passages shown in figure 6 and provides the structural integrity, alignment and positioning required to join the two turbine frames. The four coolant plenums were fed independently; each one having its own throttling valve and flow measuring orifice. As originally conceived the coolant flow was injected normal to the primary flow direction. This scheme led to penetration distances that were too great and the infusion system was modified based upon slot injection data obtained in a small flat plate tunnel. The angle between the coolant flow and the primary flow was reduced to 11° to 16° as shown in figure 6. The resulting temperature profile was then close to the desired typical profile and was considered acceptable. Test points for this experiment were taken at the conditions shown in table I both with and without the CERTS coolant flow.

Instrumentation

The turbine instrumentation locations are shown in figures 5 and 6. Turbine inlet temperature upstream of the CERTS slots was measured with 20 thermocouples, 5 on each of the 4 inlet struts. The inlet static pressure was measured with 10 static taps, 5 each on the hub and tip walls located at the inlet survey plane. Also at this plane were two small shielded total temperature probes and one total pressure probe mounted in actuators for radial surveys of inlet total pressure and temperature. The pressure probe's stem was electrically insulated from the turbine casing so that probe contact with the hub wall could be detected. The probe tip was a 0.5 mm tube flattened to 0.35 mm.

The turbine exit plane instrumentation consisted of six static taps each on the hub and tip walls and four combination probes like those shown in figure 7. These probes were mounted in self-aligning actuators and were used for radial surveys of exit flow angle, total temperature, and total pressure.

The average inlet total temperature was calculated from measured average upstream temperature and primary air flow and CERTS temperature and air flow. The exit average total temperature was calculated from the average inlet value and the turbine specific work. Inlet and exit average total pressure were calculated from continuity using these temperatures and measured air flow, static pressure, and the exit flow angle.

Three touch probe type clearance measuring devices were used to measure rotor tip clearance during testing. The laboratory ESCORT digital data acquisition system was used to record the test data and provide on-line data processing.

Analytical Method

The inviscid rotational flow code used to obtain the analytical results was developed by J. D. Denton of Cambridge University as a three-dimensional time-marching solver of the unsteady Euler equations in finite-volume form for fixed or rotating turbomachinery blade rows (ref. 2). The code assumes adiabatic blade and endwall surfaces. Non-uniform grid generation was utilized to obtain good resolution of the blade profiles. The grid dimensions for the stator vane channel were 19 pitchwise, 19 spanwise, and 58 streamwise. The grid dimensions for the rotor blade channel were 10 pitchwise, 19 spanwise, and 68 streamwise. A two-level multigrid technique was used to reduce computation time. The code was first run for the stator with the measured inlet temperature and pressure profiles from the experiment, both with and without CERTS, that are shown in figures 8 and 9. The stator exit velocity was matched to the experimental data by specifying appropriate static pressures at the stator exit hub and tip. The computed results at the stator exit were then circumferentially averaged using mass flow weighting and used as inlet conditions for the rotor. The rotor exit velocity was matched to the experimental data by specifying appropriate static pressures at the rotor exit hub and tip. The computed results at the rotor exit were also circumferentially averaged to allow comparison with the experimental survey results obtained from probes in the stationary frame.

RESULTS AND DISCUSSION

Analytical Results

The computed results for the analysis of temperature profile distortion with the nonuniform inlet temperature radial profile are presented in detail below. The uniform profile was obviously not affected by any distortion.

The computed absolute total gas temperature contours in a cross-channel plane at the vane leading edge are shown in figure 10(a). The contours are circumferentially uniform but show the radial inlet temperature profile used as the upstream boundary condition. Figure 10(b) shows the contours at the vane trailing edge plane, where hot fluid from the mean has been convected to the hub and tip corners on the pressure surface by secondary flow. The tip corner experiences a gas temperature rise of 40 K from 635 to 675 K. The hub corner has a much greater rise of 95 K from 610 to 705 K; the gas temperature rise along the hub endwall is also much greater than that along the tip endwall. The affected region on the hub endwall extends out to midpitch. The gas temperature on suction surface shows approximately the same profile at the trailing edge plane as at the leading edge plane. Figure 11 shows the computed secondary flow vectors at the vane midchord cross-channel plane. These vectors are computed as vector deviations from the grid lines, but should approximate true secondary flow vectors as long as the grid lines approximate the true streamlines. The strong secondary flows from the mean into the hub and tip corners on the pressure surface create the gas temperature rises shown in figure 10(b). Figures 12(a) and (b) show contours along the vane pressure and suction surfaces which are consistent with the previous figures.

The relative gas temperature contours at the blade leading edge plane are shown in figure 13(a). The contours at this cross-channel plane are not circumferentially uniform, although the upstream boundary condition was a circumferentially averaged radial temperature profile obtained from the results at the stator exit. Strong leading edge effects are distorting the flow in this region and subsequently affecting the temperature distribution. Figure 13(b) shows the contours at the blade trailing edge plane, where distortion similar to that shown at the vane trailing edge plane occurs. The tip corner on the pressure surface has a 50 K rise from 580 to 630 K. The hub corner has a 55 K rise from 550 to 605 K. The secondary flow vectors shown in figure 14 support the redistribution shown in figure 13(b). The contours along the pressure and suction surfaces, shown in figures 15(a) and (b), are consistent with those shown in figures 13(a) and (b) but an anomaly occurs at the hub leading edge on the pressure surface. Figure 15(b) also shows a slight contraction of the hot mean region along the suction surface. This is consistent with the secondary flow vectors shown in figure 11 that move in toward the mean along the suction surface.

Lakshminarayana (ref. 5) has presented a method of predicting rotation of isothermal surfaces in turbomachinery blade passages based upon the vorticities generated by velocity, pressure, and temperature gradients. The results presented in reference 5 predict temperature rises at the hub and tip corners of the suction surfaces of both a stator and a rotor, and would correspond to secondary flow directions opposite to those shown in figures 11 and 14. However, the inlet radial temperature gradient used in reference 5 was much greater than that used in this investigation; the streamwise vorticity induced by the large temperature gradient overwhelmed the vorticity of the opposite

sense induced by the velocity gradient. The secondary flow shown in figures 11 and 14 indicates the predominance of velocity gradient induced vorticity over temperature gradient induced vorticity for the case used in this investigation.

Comparison of Analytical and Experimental Results

The temperature and pressure profiles that were measured at the inlet survey plane shown in figure 6 were used as input conditions for the flow code in the analytical part of this study and are shown in figures 8 and 9.

Figures 16(a) and (b) compare the analytical and experimental rotor exit temperature profiles with and without CERTS. The analytical results were obtained by circumferentially averaging the computed absolute temperature using mass flow weighting at a location corresponding to the exit survey plane shown in figure 6. The profiles shown in figure 16(a) indicate that the CERTS temperature profile is mixed out at the exit survey plane, although the analytical profile is not as fully mixed out as the experimental profile is, since viscous effects were not included in the flow code. The slight temperature drop in the experimental profile at the tip endwall can be attributed to heat transfer through the casing. The profiles shown in figure 16(b) show very close agreement without CERTS, except for the previously mentioned temperature drop at the tip endwall.

Figures 17(a) and (b) compare the analytical and experimental rotor exit angles with and without CERTS. The analytical results were obtained by circumferentially averaging the computed results as mentioned above. The analytical and experimental profiles with CERTS show close agreement in the hub region, but show large differences at the mean and tip. The analytical profile shows several trend reversals from hub to tip that do not match the experimental profile, which has severe underturning from the mean to the tip. The profiles shown in figure 17(b) without CERTS show trends similar to those with CERTS but with better agreement at the tip. The poor agreement at the tip with CERTS is caused by the increased clearance due to the CERTS coolant flows. The average clearance without CERTS was approximately 0.5 percent while the average clearance with CERTS was 1.1 percent. The experimental profiles with and without CERTS are in close agreement with each other from the hub to the mean. The analytical profiles show the same trends with and without CERTS but the profile with CERTS has larger extreme values. Neither of the analytical profiles show the severe underturning at the mean that occurs both with and without CERTS; this may be caused by viscous effects that were not included in the inviscid rotational flow code.

SUMMARY OF RESULTS

Analytical and experimental results were obtained for a typical nonuniform inlet radial temperature profile through an advanced single-stage axial turbine and compared with the results obtained for a uniform profile. The three-dimensional inviscid rotational flow code used for the analysis predicted gas temperature rises at the stator vane hub and tip corners on the pressure surface of 95 and 40 K, respectively; temperature rises of 55 and 50 K were predicted at the same locations in the rotor. These predicted temperature rises were consistent with the computed secondary flow vector patterns, which would convect hot fluid from mean to the hub and tip corners on the pressure sur-

faces. The circumferentially averaged rotor exit temperature profile from the analysis agreed well with the experimental results; the CERTS temperature profile was shown to be mixed out at the rotor exit survey plane. The experimental rotor exit angle profiles indicated severe underturning at the mean both with and without CERTS; this underturning was continued from the mean to the tip with CERTS, but the profile without CERTS returned close to design at the tip. The underturning at the tip with CERTS was due to the increased clearance caused by the CERTS coolant air; otherwise, the two experimental profiles were in close agreement from hub to mean. The analytical profiles did not show the underturning at the mean that occurred both with and without CERTS; this may be caused by viscous effects that were not included in the inviscid rotational flow code.

REFERENCES

1. Cochran, R. P.; Norris, J. W.; and Jones, R. E.: A High-Pressure, High-Temperature Combustor and Turbine-Cooling Test Facility. NASA TM X-73445, 1976.
2. Denton, J. D.: An Improved Time-Marching Method for Turbomachinery Flow Calculation. ASME Paper 82-GT-239, Apr. 1982.
3. Whitney, W. J.; Stabe, R. G.; and Moffitt, T. P.: Description of the Warm Core Turbine Facility and the Warm Annular Cascade Facility Recently Installed at NASA Lewis Research Center. NASA TM-81562, 1980.
4. McDonel, J. D.; Hsia, E. S.; and Hartsel, J. E.: Core Turbine Aerodynamic Evaluation: Design of Initial Turbine. NASA CR-2512, Feb. 1975.
5. Lakshminarayana, B.: Effects of Inlet Temperature Gradients on Turbomachinery Performance. ASME Paper 74-GT-57, Mar. 1974.

TABLE I. - TURBINE TEST CONDITIONS

	Test	Standard-air equivalent
Inlet total temperature, T_o', K	672.2	288.2
Inlet total pressure, p_o', Pa	3.103×10^5	1.013×10^5
Mass flow, w, kg/sec	6.130	3.098
Specific work, h, J/kg	1.299×10^5	5.630×10^4
Rotative speed, N, rpm	11 373	7475
Total pressure ratio, p_o'/p_2'	2.360	2.408

TABLE II. - TURBINE STATOR GEOMETRY

Mean diameter, d_{mv}, cm	46.744
Mean vane pitch, s_{mv}, cm	5.648
Vane height, b_v, cm	3.564
Axial chord, c_{xv}, cm	3.556
Axial solidity, c_{xv}/s_{mv}	0.630
Aspect ratio, b_v/c_{xv}	1.000
Number of vanes	26
Leading edge radius, cm	0.508
Trailing edge radius, cm	0.089

TABLE III. - TURBINE ROTOR GEOMETRY

Mean diameter, d_{mb}, cm	46.744
Mean blade pitch, s_{mb}, cm	3.059
Blade height, b_b, cm	3.564
Axial chord, c_{xb}, cm	3.302
Axial solidity, c_{xb}/s_{mb}	1.079
Aspect ratio, b_b/c_{xb}	1.077
Number of blades	48
Leading edge radius, cm	0.305
Trailing edge radius, cm	0.089

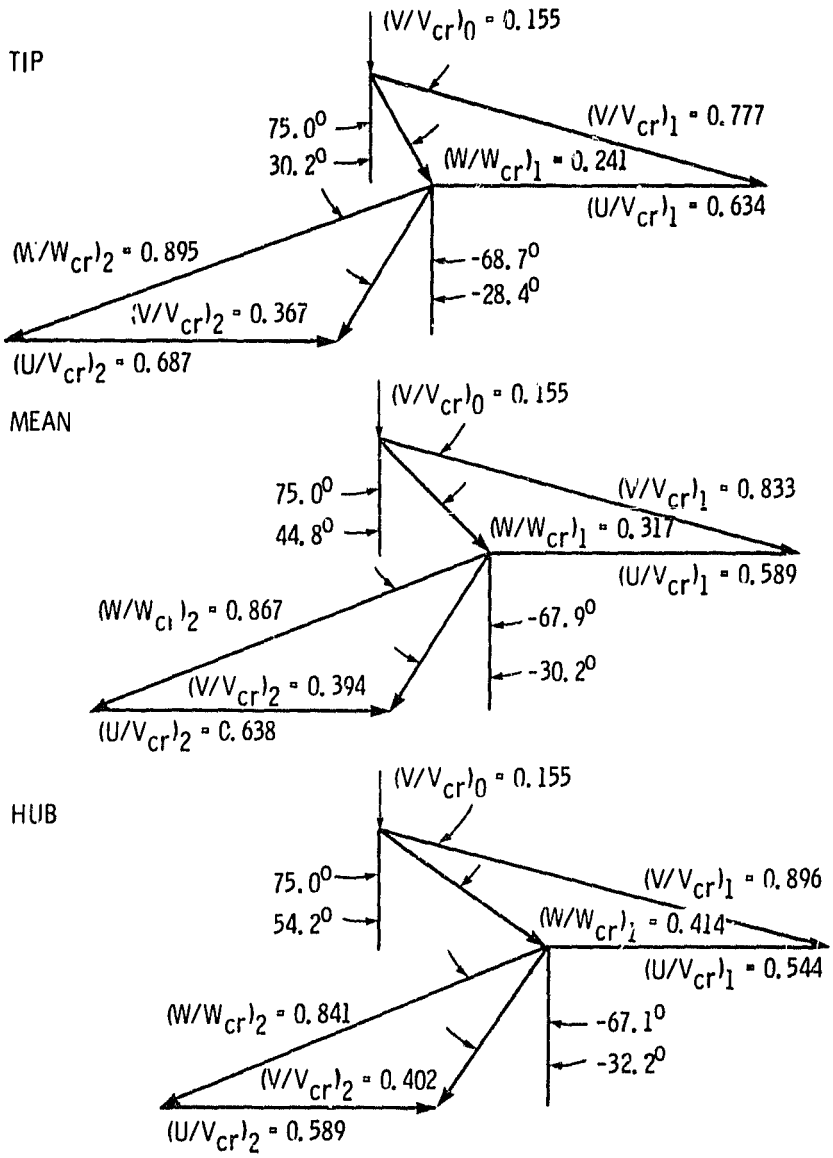

Figure 1. - Turbine design velocity diagrams.

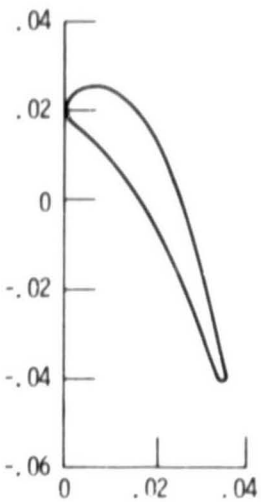

Figure 2. - Stator vane profile (dimensions in meters).

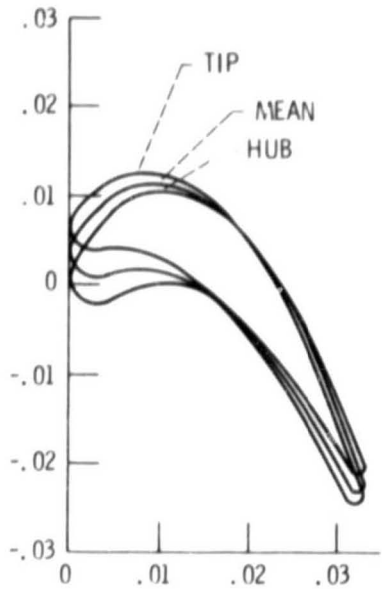

Figure 3. - Rotor blade section profiles (dimensions in meters).

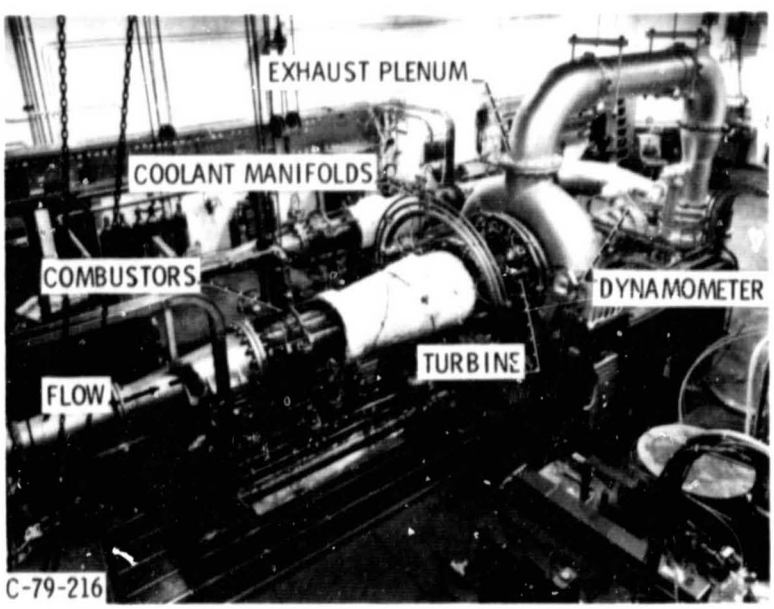

Figure 4. - Warm core turbine test facility.

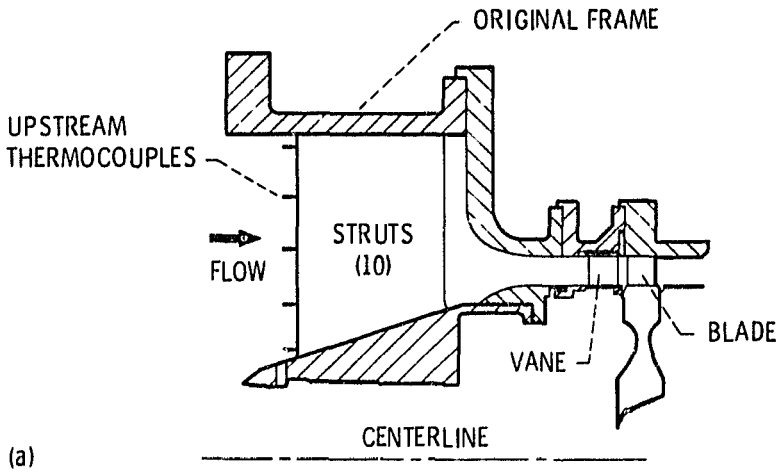

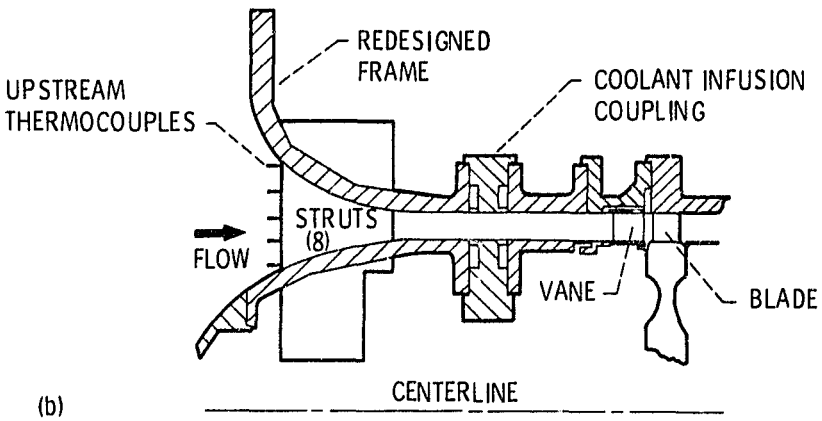

(a) Original inlet section.
(b) CERTS inlet section.

Figure 5. - Turbine cross-sectional views.

"Page missing from available version"

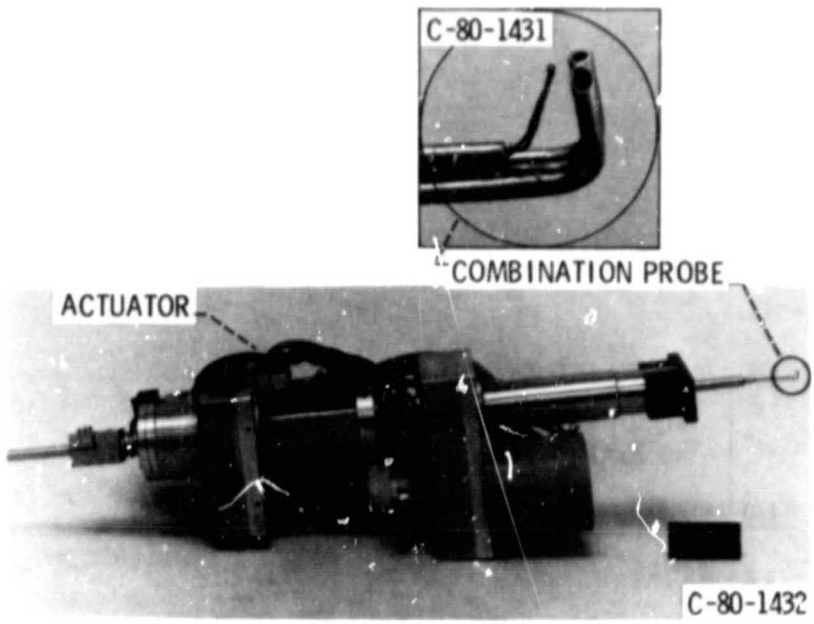

Figure 7. - Rotor exit survey probe.

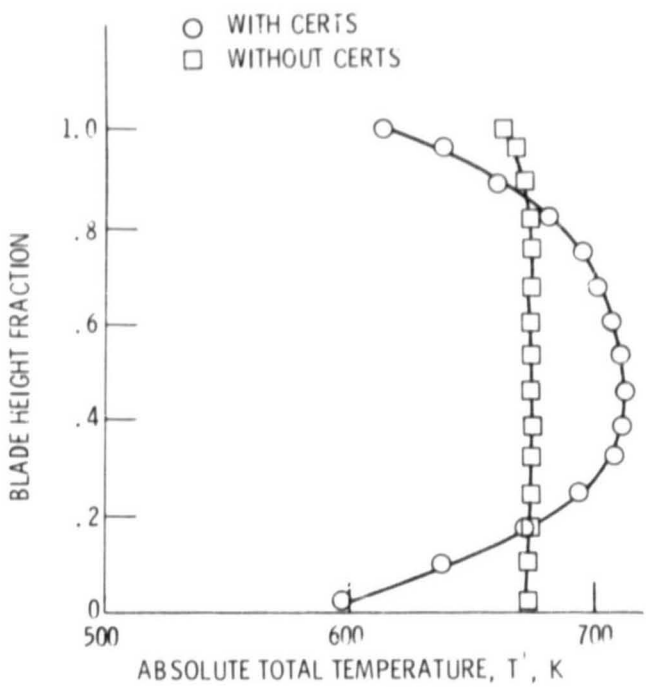

Figure 8. - Stator inlet temperature profiles.

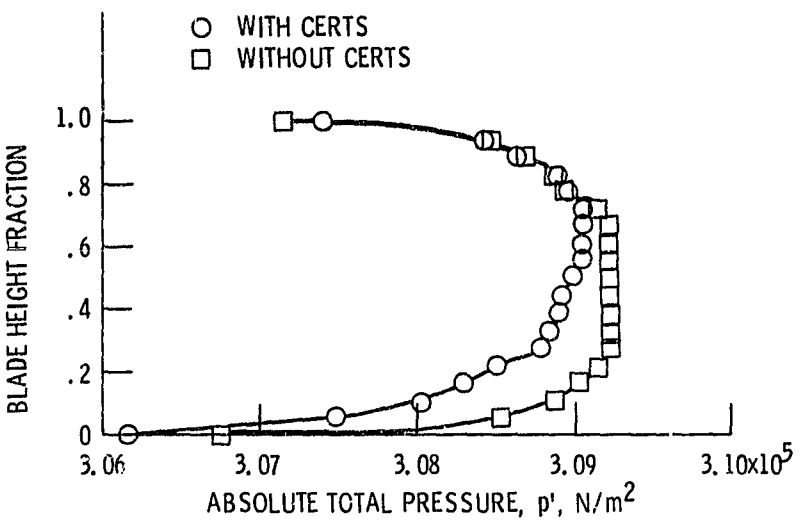

Figure 9. - Stator inlet pressure profiles.

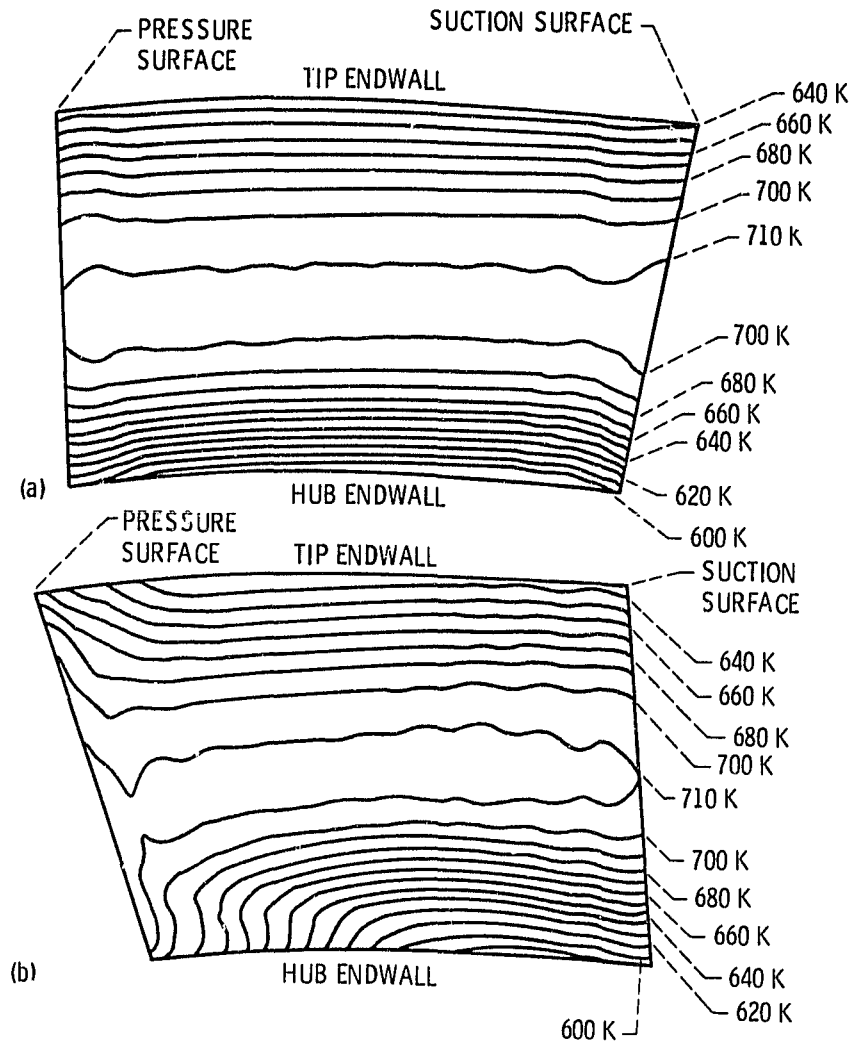

(a) At stator vane leading edge.
(b) At stator vane trailing edge.

Figure 10. - Computed absolute total gas temperature contours.

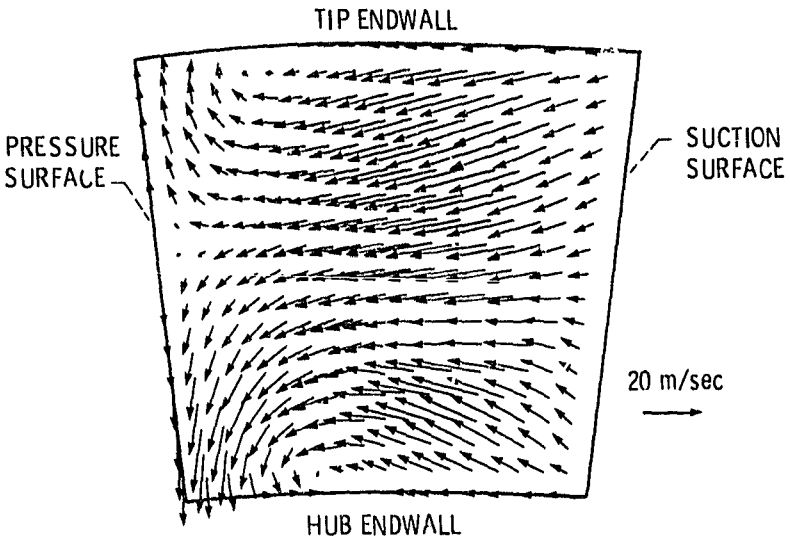

Figure 11. - Computed absolute secondary flow vectors at stator vane mid-chord.

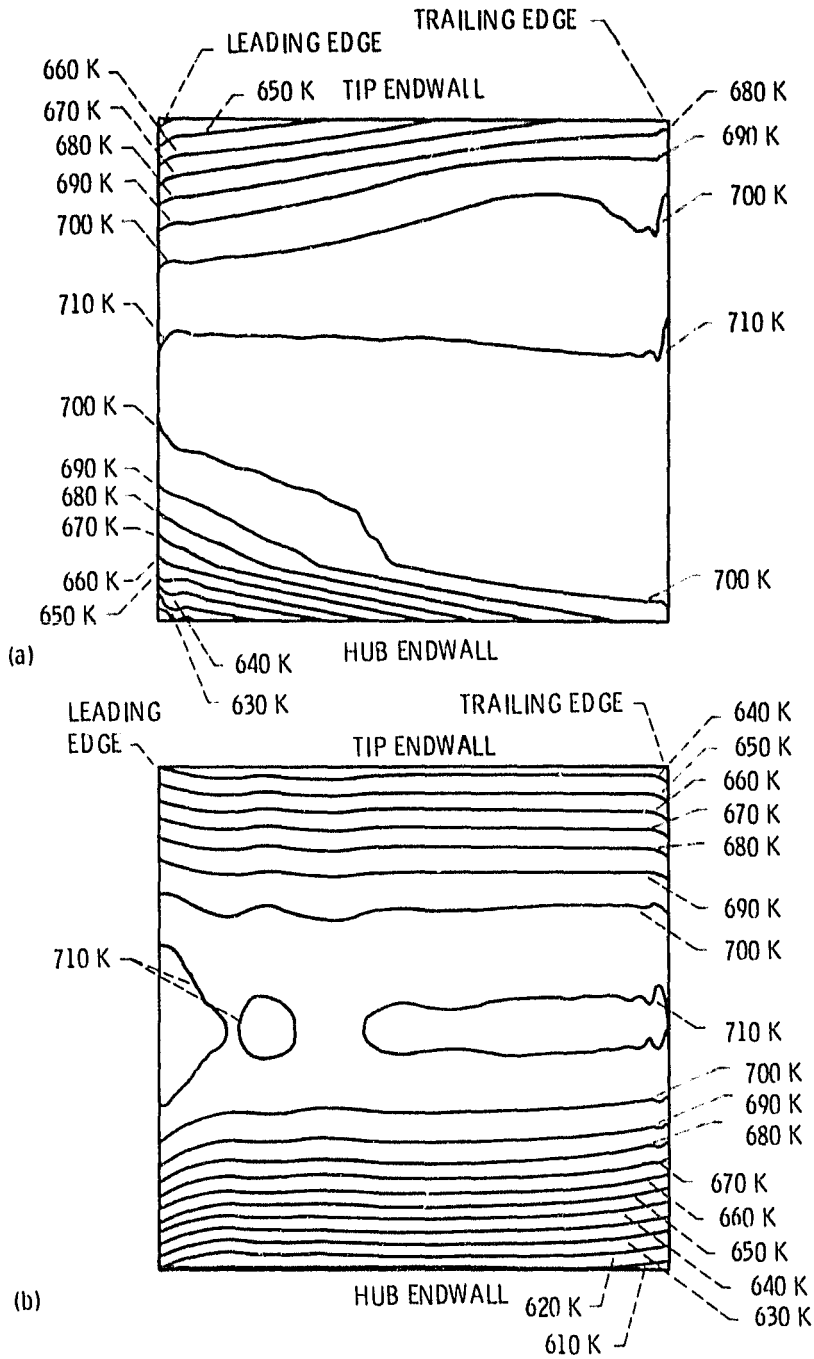

(a) At stator vane pressure surface.
(b) At stator vane suction surface.

Figure 12. - Computed absolute total gas temperature contours.

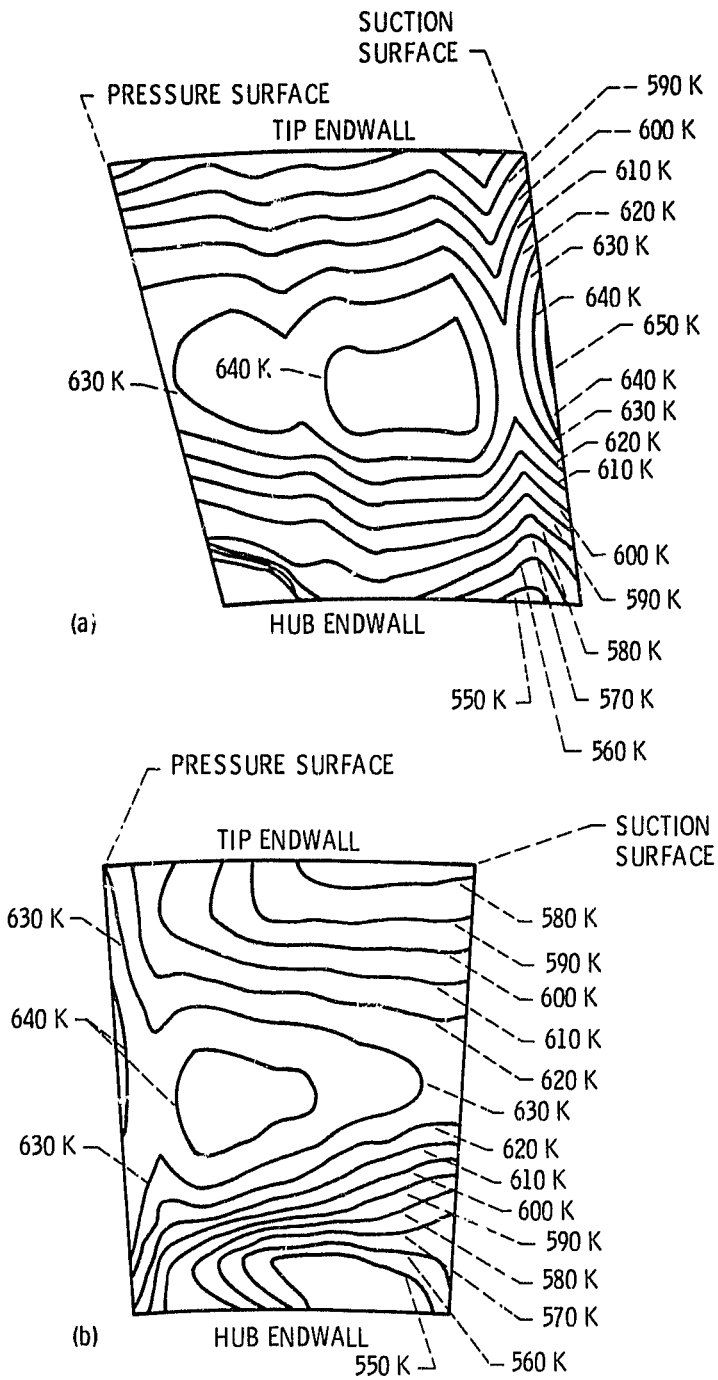

(a) At rotor blade leading edge.
(b) At rotor blade trailing edge.

Figure 13. - Computed relative total gas temperature contours.

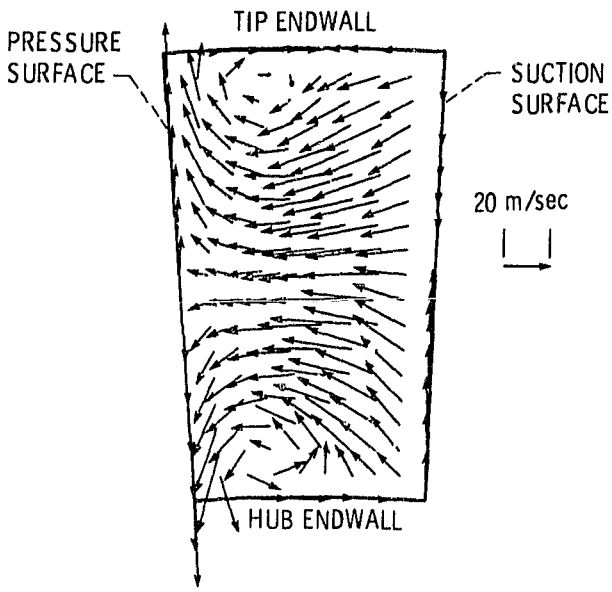

Figure 14. - Computed relative secondary flow vectors at rotor blade mid-chord.

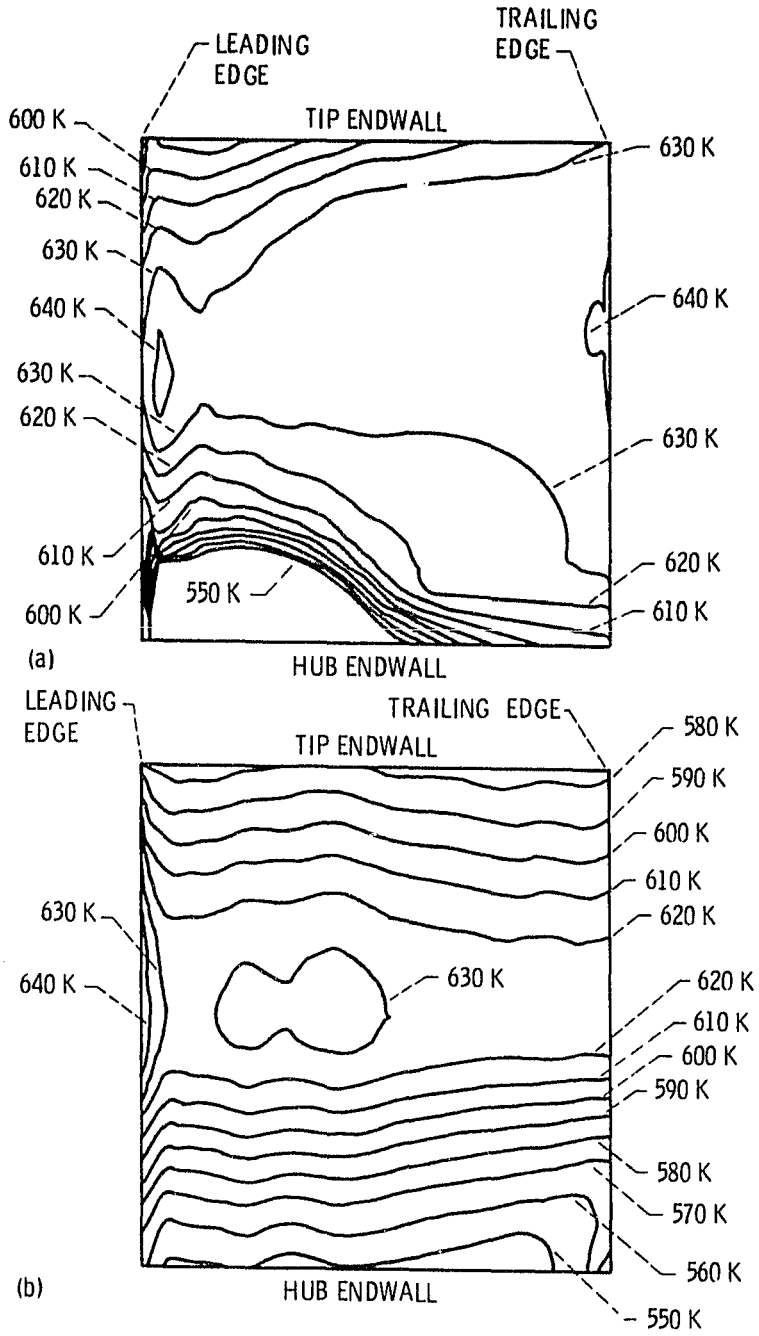

(a) At rotor blade pressure surface.
(b) At rotor blade suction surface.

Figure 15. - Computed relative total gas temperature contours.

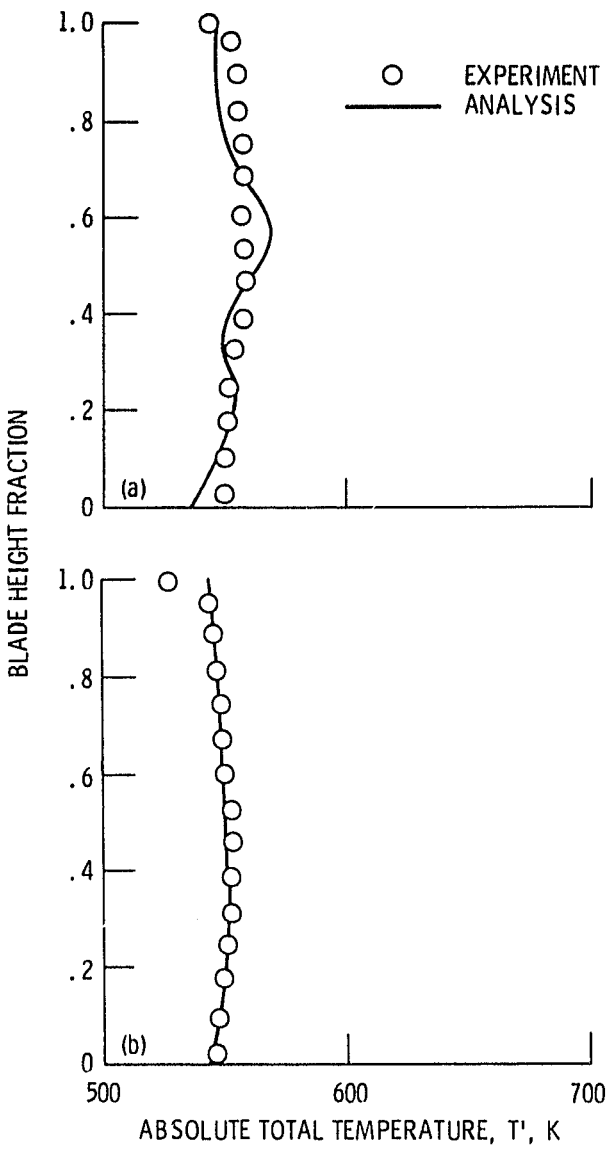

(a) With CERTS.
(b) Without CERTS.

Figure 16. - Rotor exit temperature profiles.

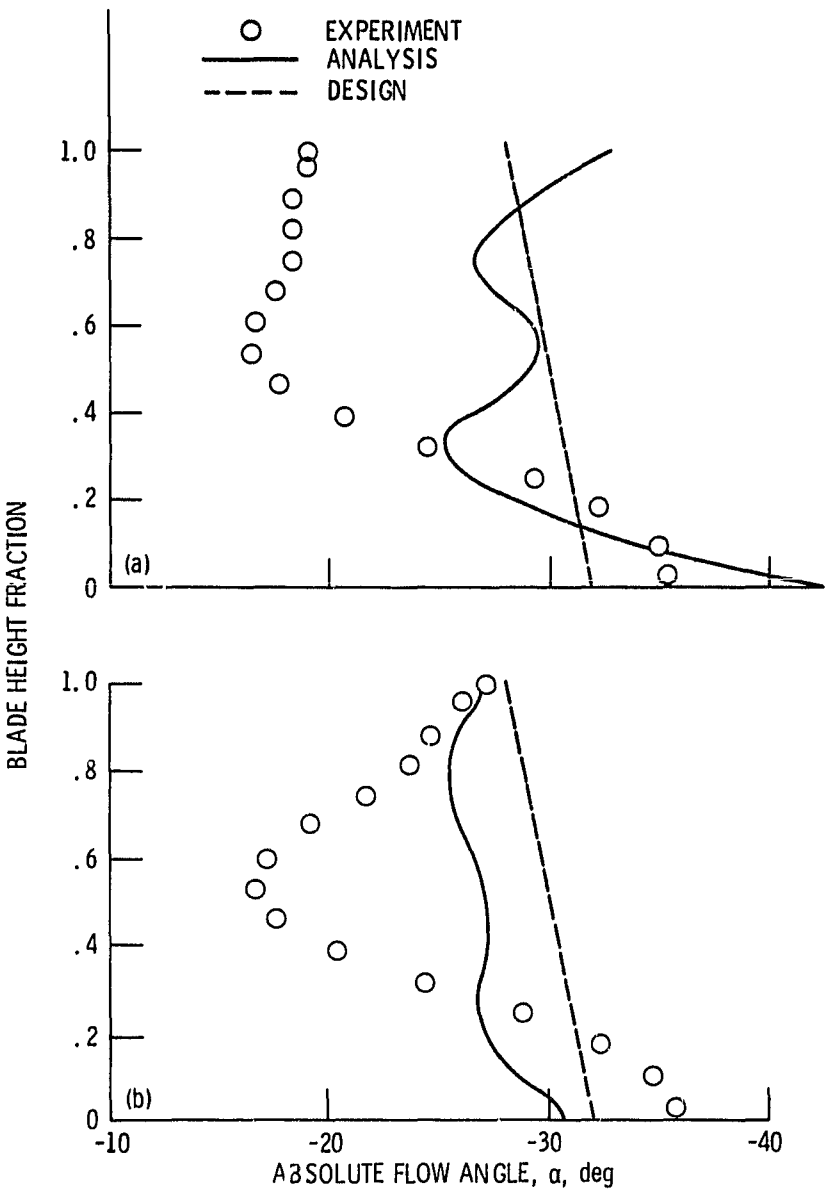

(a) With CERTS.
(b) Without CERTS.

Figure 17. - Rotor exit flow angle profiles.